Pore Fluid Reactivation of Normal and Reverse Faults

By: Nicholas Caviglia

Advisors: Dr. Wenlu Zhu and Dr. Melodie French

Abstract

With the rise of hydraulic fracturing and the ever increasing need for waste water disposal determining where to dispose of waste water is a significant issue. With record numbers of earthquakes in Oklahoma due to waste water injection it is clear that the hazards of waste water injection are not fully understood. A step to understanding what is happening in Oklahoma and other places is to investigate the effects of pore fluid pressure on normal and reverse faults. Different styles of faulting were found to occur between normal faults and reverse faults. Pore pressure jumps are found to occur during normal faulting but not during reverse faulting. These pore pressure jumps only occur when there is active fluid injection and the strength of the signal is related to the rate of injection of the pore fluid.

Introduction

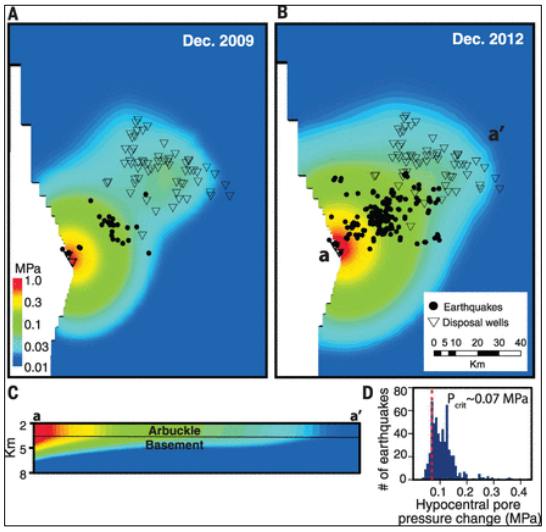

Figure 1 Locations of earthquakes and disposal wells are shown in relation to the amount of pore pressure change over the area. It was found that and average increase of 0.07 MPa triggered earthquakes (Keranen 2014).

The central United States experienced a rapid increase in earthquakes starting in 2008 (Figure 1). waste water disposal from unconventional hydrocarbon production is proposed to cause. Seismicity in Oklahoma has increased by forty-fold between 2004 and 2008 compared to 1976 to 2007(Keranen 2014).

Pore fluid pressure is the cause of this increase of seismicity. Pore fluid pressure allows faults to reactivate more easily and the greater the increase of pore fluid pressure the smaller amount of stress needed to cause an earthquake.

How pore increasing pore fluid pressure affects specific styles of faulting remain unknown. For example are normal faults or reverse faults affected differently? Does the rate of pore fluid injection make a difference in faulting style? Both faulting style and pore fluid injection rate play an important role in slip behavior along a fault

Background

There are two different types of stress which are normal stresses and shear stresses. Principal stresses are perpendicular to the faces of the volume of material while shear stresses are parallel to these faces.

The magnitude and orientation of the principal stresses determines the type of faulting that an area will experience. Normal faults are found in areas of geologic extension, while reverse faults are found in areas of geologic shortening. In a reference frame relative to the surface of the Earth, the direction of movement is opposite for normal and reverse faults. In a normal fault he hanging wall moves down relative to the foot wall of the fault However, for a reverse fault the hanging wall moves up the foot wall.

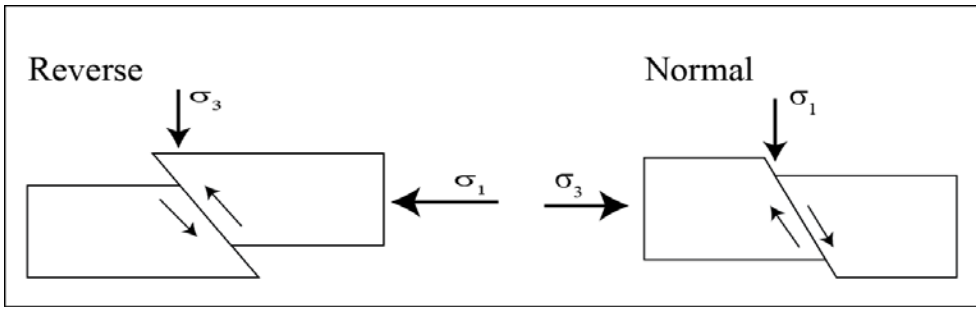

Figure 2 Main principal stresses for normal and reverse faults. For normal faults the maximum principal stress is in the vertical direction while it is in the horizontal direction for reverse faults.

This difference in faulting styles is based off of fault mechanics and depends on the direction of the maximum principal stress. As shown in (Figure 2), the maximum principal compressive stress, σ_1, for reverse faults comes from the horizontal direction and is caused by compressional tectonic forces Normal faults maximum principal stress is in the vertical direction. This force in nature relates to the overburden caused by the burial of the fault.

During brittle fracture, rocks undergo four main stages of faulting (Paterson and Wong, 2005). The first stage cracks in the rock will seal. In this stage a precut sample will begin to behave as a solid rock. The second stage is marked by the rock accommodating stress elastically. While the rock is behaving elastically a large increase in differential stress does not correlate to a large amount of strain; also if the differential stress is removed the rock will return to its original shape. Stage three occurs when the rock can no longer behave elastically and begins plastic deformation. Plastic deformation begins the rock cannot resist any further increase in differential stress permanently changing its shape to accommodate this increase. Or, in the case of a previously faulted rock there will be creep along the fault surface. The fourth and final stage is shown by the relieving of stress by the fracturing of the rock, a precut sample will quickly slide along the fault surface (Paterson and Wong, 2005).

Changes in tectonic stresses can cause slip along the fault this is known as fault reactivation Pore pressure reduces the amount of shear stress needed to reactivate a fault. Pore fluid pressure comes from fluid in the pore space of a rock. If the pore space is full with fluid stress that is applied to a rock is somewhat offset by the pore fluid pressure. The stress that is holding the fault together is also offset by the pore fluid pressure, which effectively decreases the normal principal stress on the fault allows the fault to reactivate with a lower shear stress compared to a fault with no pore fluid pressure (Hubbert and Rubey, 1959).

Mohr's stress diagrams visually repersent the relationship between principal stresses, normal stresses, and shear stresses. Normal stress is along the X-axis and shear stress is along the Y-axis. The circles on a Mohr's stress diagram repersent the stress state of a material. The center of the circle repersents the effective mean stress of the sample. The diameter of the circle repersents the differential stress on the material. The circumfrince of the circle shows the stress state for any given angle of a plane through the rock. The failure criteria line shows the stress state at which a material will slide along the fault surface. The slope of the failure criteria line refered to as the coefficient of friction and is a material property. If the material has not been previously fractured the failure criteria line intersects the Y-axis at some distance above the orign, based on the amount of stress required to initally fracture the material. However, all of the samples used in the following experiments have been precut so the failure criteria line will intersect the origin. In (Figure 3) it can be seen that reverse faults require a larger change in stress to reactivate than normal faults.

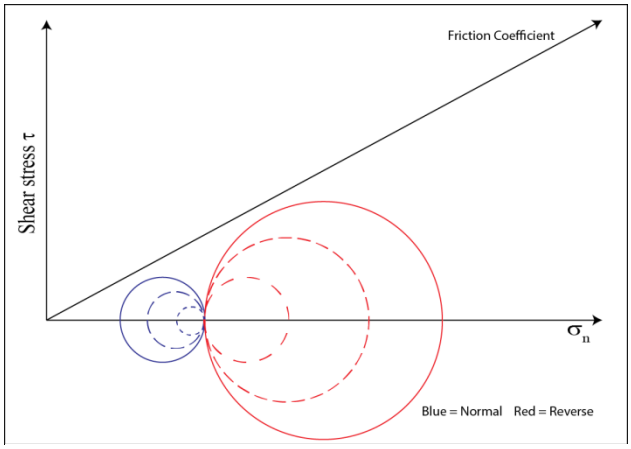

Figure 3 Circles shows overburden remaining constant while tectonic stress increases. The series of blue circles shows overburden

Pore pressure translates the circles on a Mohr's stress diagram to the left without changing the size of the circle. This translation happens because pore fluid pressure decreases the average stress in a material.

Hypothesis

My hypothesis is that fault slip behavior will be different between normal and reverse faults. The reasoning behind this hypothesis is as follows. Rocks will start to behave plastically when the differential stress that they are under is a certain proportion of the differential stress required to completely fracture the rock. In a pre-cut sample like the ones used in these experiments the samples creep along the fault.

Experimental Design

To test this hypothesis, I conducted experiments under four sets of conditions were run in two different sandstones. The experiments simulated normal and reverse faulting stress paths under different pore fluid conditions, including fluid injection at different rates, one set at a higher injection rate than the other set. Each type of experiment was run twice, changing rock type between experiments. The use of two different rock types tests to see if any phenomena observed is a factor of a specific rock type. Comparing rapid injection to no or slow injection was used to determine if the rate of injection mattered in fault kinematics The experiment uses one of two types of saw-cut, porous sandstone samples. The two rock types are Berea and Darley Dale sandstone. Berea is a quartz arenite with a porosity of around 20% and the Darley Dale is an arkose with a porosity of around 13% (Zhu and Wong 1997). The fact that the porosity is so high allows the samples to be easily saturated and for pore pressure to distribute thorough the

sample rapidly. Samples must be fully saturated so that the effects of pore fluid pressure can be transmitted throughout the entire sample. The saw cut runs through the samples at a 30 degree angle to the core axis. This saw acts as a preexisting fault that will be reactivated during the experiment. A pre-cut sample aids in the reproducibility of the fault structure. Similar fault structures leads to similar mechanical data.

For the reverse faulting experiments the first step is to bring the confining pressure $Pc = \frac{\sigma 1+\sigma 2+\sigma 3}{3}$ up to 65 MPa. Once this pressure is reached the confining pressure is held constant. The pore pressure is then raised to 10 MPa. After the pore pressure is raised to its starting position the samples axial stress is increased by a hydraulic piston which provides differential stress (Figure 4). The differential stress is increased until the sample begins to behave plastically and slip begins along the fault. The pore pressure is then raised steadily until the end of the experiment. Experiments with no increase in pore fluid pressure are only stressed axially.

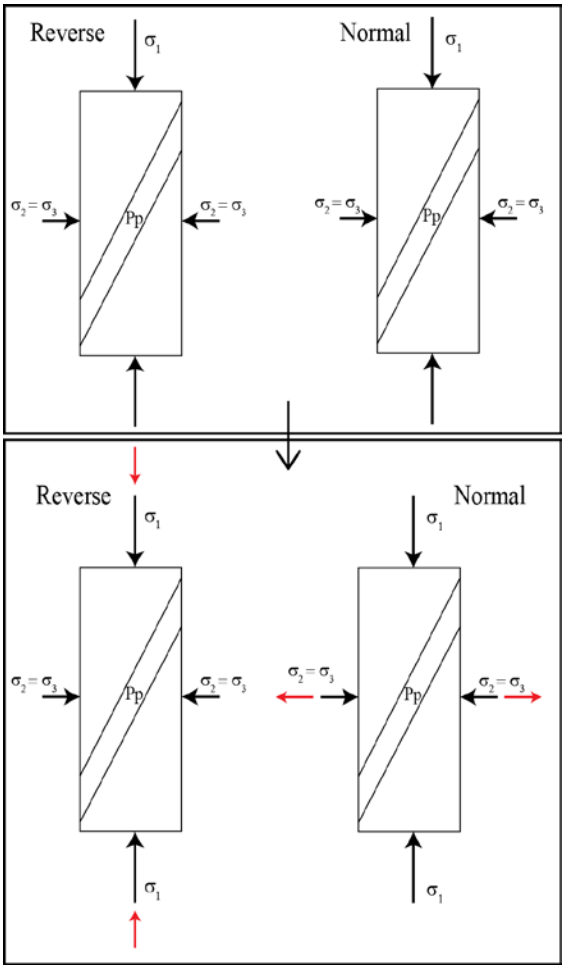

Figure 4 Experimental set up of stress for normal and reverse faults

The first step of the normal faulting experiments is increasing the confining pressure to 65 MPa. Once the confining pressure is reached the axial stress is increased until the samples behave plastically and there is creep along the fault. The axial stress is then stopped and the confining pressure is lowered. While the confining pressure is being lowered the pore fluid pressure is raised, in the experiments that require it.

A saw cut sample is selected, and weighed. The sample is then saturated in distilled water under a vacuum which assists in the removal of any air that may be in the pores. After the sample has been saturated it is removed from the vacuum and weighed again. The two halves of the sample are then put together and inserted into a shrink wrap tube. Spacers are then placed in each end of the tube and then the sample and spacers are mounted on the end cap that is attached the bolt that will be inserted into the tri-axial deformation machine. The other end cap is then inserted. The third layer of shrink wrap is placed over the first two and then heated. Wire rings are attached to the top and bottom sample. Finally the sample is screwed into the apparatus. After the experiment is run confining pressure is lowered, the Piston is retracted, and the sample is removed, dried, taken off the end caps and stored.

Calibrations

Sensor	Range and Precision
confining pressure:	345 ± 0.9 MPa (50,000 ± 125 p.s.i.)
main ram displacement:	154 ± 0.8 mm (6 ± 0.03 in)
load cell-main ram:	3647±4 MPa (529,000 ± 500 p.s.i.)
pore fluid pressure:	69±0.08 MPa (10,000 ± 11 p.s.i.)
pore volumometer:	61.86±0.31 cm3 (3.775 ± 0.019 in3)
strain gauge:	350 ± 1.05 ohm

Table 1 Range and precision of the various sensors on the tri-axial deformation apparatus

Four sets of voltages are outputted by the tri-axial deformation machine and they are the load on the load cell, axial displacement, confining pressure and pore fluid pressure. These raw voltages are produced in three different ways. The voltage that corresponds to axial displacement is measured by a Linear Variable Differential Transducer (LVDT). LVDTs consist of two coils of wire wrapped around one another and a magnetic rod. The inner coil of wire has an oscillating voltage applied to it, the introduction of the magnetic rod couples the inner and outer coils. Coupling the coils induces a voltage on the second coil and as the magnetic rod moves further through the inner coil this voltage changes. To calibrate a LVDT the magnetic rod was pushed through the inner coil at a constant rate. The corresponding voltages were recorded and the slope of this line gives the change in voltage per distance. A LVDT is used to measure the axial displacement. The voltages that correspond to the confining pressure and pore fluid pressure are measured with a pressure transducer. The pressure transducer has two main parts, a strain gage affixed to a diaphragm that responds to pressure. The amount the strain gage reads is dependent on how much the diaphragm, which has been calibrated in the factory deforms. The load cell uses four strain gages connected in a simple circuit to output a voltage that corresponds to the load on the load cell. The precision of the different sensors is shown in (Table 1) (Tamarkin 2011).

The error on the load cell comes from the fact that the piston which is attached to the load cell passes through an O-ring that seals the confining pressure chamber. However, if the main ram is being pushed steadily in one direction this error becomes unimportant to each individual experiment and will only come into play when comparing experiments. The experiments that are proposed will only require the main ram to move in one direction during the experiment.

Data is collected from when the sample is inserted into the machine until the experiment is over. The raw data that is gathered is in the form of voltages. These voltages are recorded every half second by a computer. The raw voltages are imported into Excel and then filtered with a MATLAB script to smooth the data. The filter works in such a way that it removes high frequency electrical noise but leaves the overall trend of the data intact. The filtered voltages are turned into their corresponding measurements using a predetermined set of equations. These measurements can then be further analyzed and processed. A common way of looking at this sort of data is a graph that shows friction coefficient verses axial displacement or time.

Results

The primary difference between experiments was faulting style and the data for these types of experiments is visibly different. Reverse faulting experiments have many times the amount of displacement as the normal faulting experiments. The reason behind this is that the confining pressure must be kept at least 10 MPa above the pore fluid pressure. If the pore fluid pressure exceeds the confining pressure the shrink wrap jackets would burst and contaminate the confining pressure fluid. During the normal faulting experiments, the confining pressure is lowered while the pore fluid pressure is increased, limiting the amount of time that the experiment can be run. On the other hand, the confining pressure for the reverse faulting experiments is kept constant while the pore pressure is increased allowing for a longer experiment.

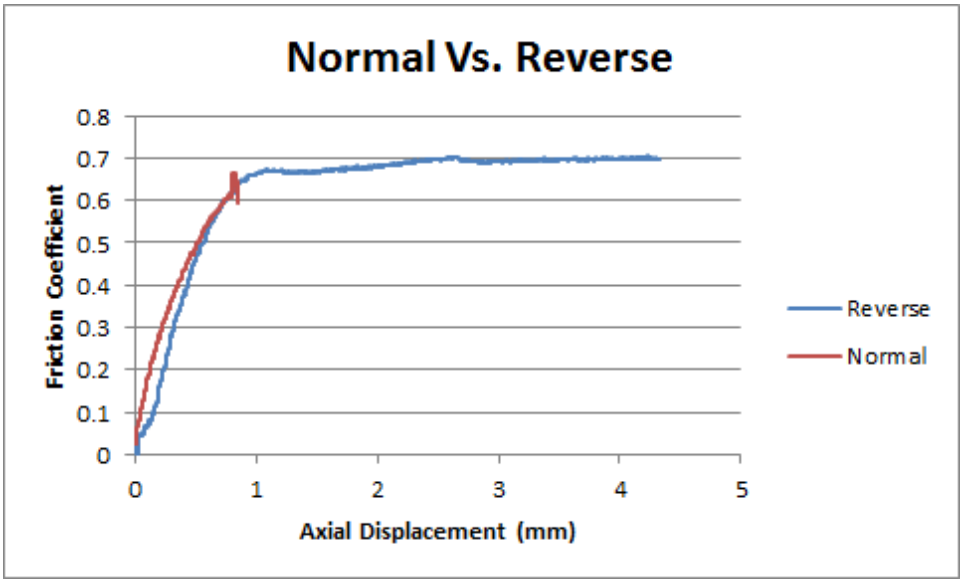

Figure 5 Friction coefficient verses axial displacement

The rate of the imposed pore pressure increase is observed in a graph of pore pressure verses time and finding the slope of a line of best fit. This graph shows a constant increase in pore pressure with time. Looking at this graph it can be determined if there are any pore pressure changes beyond those that were imposed in the data. If there was a rapid jump then the corresponding shear stress verses time graph was plotted. This data was when compiled into (Figure 6).

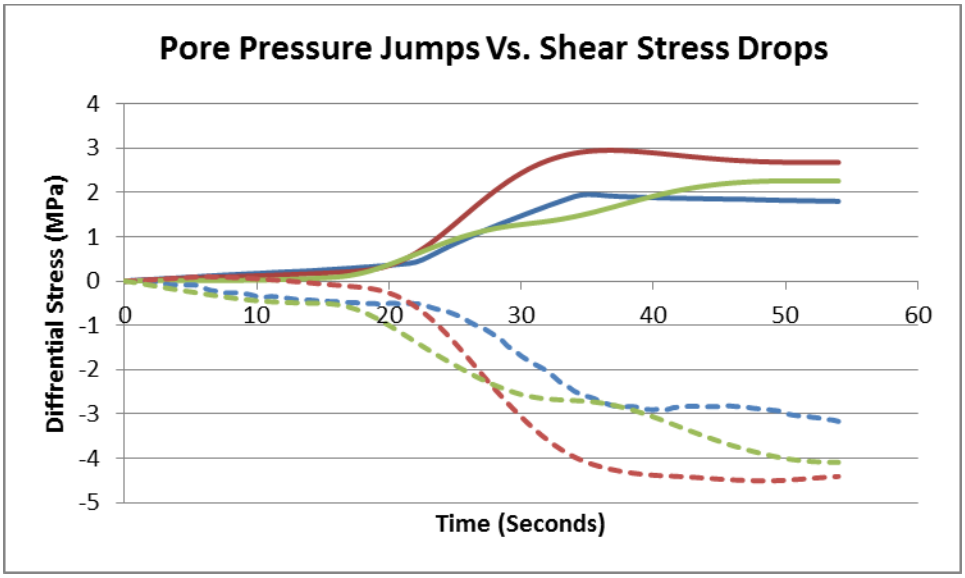

Figure 6 Solid lines show pore pressure increases while dashed lines show the associated shear stress drops. The Y-axis is the normalized change in stress. Normalization was needed because the pore pressure increases and shear stress drops occurred at different pore pressures

After the shear stress drops and pore pressure increases were graphed the magnitude of each drop and increase was recorded. The magnitudes were found by recording where the pore pressure or shear stress rates started to change until they returned to the original rate.

Experiment	Stone Type	Fault Type	Conf. Pres.	PP Rate	# of Events	AVE PPI	AVE SSD
B4_F	Berea	Normal	62	0	0	N/A	N/A
Bcut30	Berea	Normal	61	1.1	2	2.5	3.75
DD4_F	Darley Dale	Normal	62	0	0	N/A	N/A
DD1_F	Darley Dale	Normal	62	0.9	1	1.5	2.25
Bcut21	Berea	Reverse	51	0	0	N/A	N/A
Bcut22	Berea	Reverse	52	0.08	0	N/A	N/A
DD7_F	Darley Dale	Reverse	64	0	0	N/A	N/A
DD6_F	Darley Dale	Reverse	62	0.32	0	N/A	N/A

Table 2 All experiments are given a experiment number as shown by the left most column, the experimental set up is listed. The number of events refers to the number of pore pressure jumps. AVE PPI= average pore pressure increase and AVE SSD = average shear stress drop

Rapid pore pressure increases only occurred in normal faulting experiments with pore fluid injection. Normal faulting experiments without injection showed none of the rapid pore pressure increases. The rate of pore fluid injection also plays an important part in the characteristic of shear stress drops. Slower injection rates showed less pronounced shear stress drops compared to faster pore fluid injection rates and, though there were still rapid pore pressure increases these too were less pronounced. When there was no pore fluid injection there was no pore pressure increase rapid or otherwise, or associated shear stress drops in either case. In the case of reverse faults, there were no rapid pore pressure increases in any case. Shear stress was noted to drop but its decrease occurred over the time scale of minutes rather than normal fault shear stress drops that took tens of seconds. The rate of shear stress drop translates directly into the characteristics of fault movement.

Discussion

A rapid drop in shear stress correlates to rapid movement along the fault surface and slow drop in shear stress implies creeping behavior along the fault rather than a high energy release rate.

One possible reason for this behavior is as follows. As confining pressure decreases the inter-grain forces decrease allowing pore space to increase with the increasing pore fluid pressure. At some pressure the grains will shift causing rapid movement along the fault. The rapid movement along the fault and energy released in this movement causes the pore space to close, holding the pore pressure at the higher pressure. Another possible explanation is that the rapid movement along the fault changes the configuration of pore spaces causing both the immediate and prolonged increase in pore pressure.

Furthering this research requires further analysis of the data that has already been collected and collecting more data. Analyzing this data would give more information about the mechanism that cause the pore pressure jumps. Performing more experiments would allow a more complete analysis of the phenomena. Additional experiments at intermediate levels of pore fluid injection would help to better characterize the pore pressure jumps. Also additional experiments could use other stone types. Currently, only porous sandstones have been analyzed. It would be interesting to see if the same phenomena occur in rocks that are not as ideally suited to these experiments. Experiments with other rock types would also make applying this data to the real world more realistic.

Conclusion

Understanding how all types of faults react to increasing pore fluid pressure will help in the planning of where waste water wells can be placed and how fast they can inject water. The knowledge that injection along normal faults causes an increase in seismicity can be used in the future in waste water management and hazard mitigation. However, the processes are not fully understood so more research must be done.

References

Brace, W.F. and Byerlee, J.D. (1966). Stick-slip as a mechanism for earthquakes. *Science* **153**, 990-992

Hubbert, King M., and William W. Rubey. "ROLE OF FLUID PRESSURE IN MECHANICS OF OVERTHRUST FAULTING." *BULLETIN OF THE GEOLOGICAL SOCIETY OF AMERICA* 70 (1959): 115-66. Web. 17 Apr. 2014.

Paterson, Mervyn S., and Teng-fong Wong. *Experimental Rock Deformation - the Brittle Field*. Berlin: Springer, 2005. Print.

Rutqvist, J., J. Birkholzer, F. Cappa, and C.-F. Tsang. "Estimating Maximum Sustainable Injection Pressure during Geological Sequestration of CO2 Using Coupled Fluid Flow and Geomechanical Fault-slip Analysis." *Energy Conversion and Management* (2007). Web. 9 Apr. 2014. <www.sciencedirect.com>.

Scholz, C. H.. *The mechanics of earthquakes and faulting*. 2nd ed. Cambridge, UK: Cambridge University Press, 2002. Print.

Sharp increase in central Oklahoma seismicity since 2008 induced by massive wastewater injection K. M. Keranen, M. Weingarten, G. A. Abers, B. A. Bekins, and S. Ge *Science 25 July 2014: 345 (6195), 448-451.Published online 3 July 2014 [DOI:10.1126/science.1255802]*

Tamarkin, Thomas. *Progressive Microscopic Damage and the Development of Macroscopic Fractures in Porous Sandstones*. Thesis. University of Maryland College Park, 2011. Print.

W. L. Ellsworth, Science 341, 1225942 (2013). DOI: 10.1126/science.1225942

Zhu, W., *and* T. Wong *(*1997*),* The transition from brittle faulting to cataclastic flow: Permeability evolution, J. Geophys. Res., 102*(*B2*),* 3027–3041, *doi:*10.1029/96JB03282